

Efficient Action Counting with Dynamic Queries

Zishi Li¹, Xiaoxuan Ma¹, Qiuyan Shang¹, Wentao Zhu¹,
Hai Ci¹, Yu Qiao², and Yizhou Wang¹

¹ Peking University

² Shanghai Jiao Tong University

Abstract. Temporal repetition counting aims to quantify the repeated action cycles within a video. The majority of existing methods rely on the similarity correlation matrix to characterize the repetitiveness of actions, but their scalability is hindered due to the quadratic computational complexity. In this work, we introduce a novel approach that employs an action query representation to localize repeated action cycles with linear computational complexity. Based on this representation, we further develop two key components to tackle the essential challenges of temporal repetition counting. Firstly, to facilitate open-set action counting, we propose the dynamic update scheme on action queries. Unlike static action queries, this approach dynamically embeds video features into action queries, offering a more flexible and generalizable representation. Secondly, to distinguish between actions of interest and background noise actions, we incorporate inter-query contrastive learning to regularize the video representations corresponding to different action queries. As a result, our method significantly outperforms previous works, particularly in terms of long video sequences, unseen actions, and actions at various speeds. On the challenging RepCountA benchmark, we outperform the state-of-the-art method TransRAC by 26.5% in OBO accuracy, with a 22.7% mean error decrease and 94.1% computational burden reduction. Code is available at <https://github.com/lizishi/DeTRC>.

Keywords: Temporal repetition counting · Video understanding

1 Introduction

Temporal periodicity is a ubiquitous phenomenon in the natural world. Temporal Repetition Counting (TRC) aims to accurately measure the number of repetitive action cycles within a given video and holds significant potential for applications ranging from pedestrian detection [29] to fitness monitoring [11].

Pioneer methods [1, 6, 7, 16, 27, 37, 38] represent time-series video data as one-dimensional signals and employ spectral analysis techniques such as the Fourier transform. While suitable for short videos with fixed periodic cycle lengths, these methods struggle to handle real-world scenarios with varying cycle lengths and sudden interruptions. Recent studies shift to deep learning-based methods [9, 13, 17, 46] and show promising performances. Notably, most of these methods, such as RepNet [9] and TransRAC [13], utilize a temporal similarity

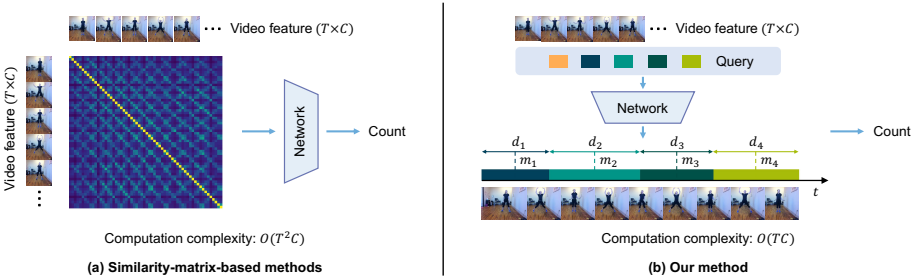


Fig. 1: Comparison of (a) similarity-matrix-based methods and (b) our proposed action query-based method. Unlike the similarity-matrix-based methods, which exhibit a quadratic growth $O(T^2C)$ in computational complexity as the length of the input video T increases, our approach is characterized by a linear growth $O(TC)$ in complexity, where C denotes the feature dimension of the video frames. This distinct advantage allows us to effectively process long videos that contain varying durations of action sequences.

correlation matrix to depict repetitiveness, as illustrated in Fig. 1 (a). Nevertheless, the computational complexity of this representation grows quadratically with the number of input frames T , highlighting a significant gap in scalability that hinders their application to real-world scenarios of varying action periods and dynamics.

Recent progress in action detection [22,33] introduces an efficient representation of action periods by associating each action instance with an action query, similar to DETR [3]. Inspired by this, we propose to formulate the TRC problem as a set prediction task where the goal is to detect every action cycle by representing it as an action query. This novel formulation reduces the complexity from quadratic to linear and enables counting long videos with varying action periods, as illustrated in Fig. 1 (b). However, directly applying the action detection approaches [22, 33, 44] to the TRC problem proves inadequate (Tab. 1) in addressing two distinctive challenges unique to TRC. These challenges underscore the complexity of TRC, highlighting why TRC is not merely another action detection task but requires a nuanced approach that considers the unique nature of repetitive actions. We highlight the two inherent differences between TRC and the classical action detection task:

1. TRC requires recognizing *open-set* action instances depending on the input video, rather than detecting predefined action classes in the detection task.
2. TRC requires recognizing action instances with *identical* content, while detection does not.

As a result, approaching TRC as a simple action detection task results in inferior performance as shown in Sec. 4.3. In contrast, we propose two novel strategies to address these challenges and redefine the framework for TRC. In response to the first challenge, we propose *Dynamic Action Query* (DAQ), which

adaptively updates the action query using distilled content features from the video encoder. This mechanism allows the decoder to attend to the “action of interest” based on the input video contents in a dynamic and contextually aware manner, without the need for manual definition. To tackle the second challenge, we propose *Inter-query Contrastive Learning* (ICL). It enforces that the repetitive action cycles are grouped together in the learned representation space while being separated apart from non-repetitive (*e.g.* background or distracting) video content. The integration of two core components (DAQ and ICL) ensures that the action instances are identified adaptively based on the video content and their contextual similarity. In other words, our queries are designed to localize the contextually similar action instances, which aligns exactly with the definition of repetition counting. Extensive experiments validate the effectiveness of the two proposed designs.

We summarize our contributions as follows:

1. We provide a novel perspective to tackle the TRC problem using a simple yet effective representation for action cycles. Our approach reduces the computational complexity from quadratic to linear and is robust to varying action periods and video lengths.
2. We propose *Dynamic Action Query* to guide the model to focus on the action of interest and improve generalization ability across different actions.
3. We introduce *Inter-query Contrastive Learning* to facilitate learning repetitive action representations and to distinguish these from distractions.
4. By addressing the scalability issue and unique challenges of TRC, our method on two challenging benchmarks notably surpasses state-of-the-art (SOTA) methods in terms of both accuracy and efficiency. Notably, our method strikes an effective balance in handling various action periods and video lengths, offering a significant leap forward in the practical application of TRC technologies.

2 Related Work

2.1 Temporal Repetition Counting

Traditional methods [1, 6, 7, 16, 27, 37, 38] frequently employ spectral or frequency domain techniques for the analysis of repetitive sequences, thereby preserving the underlying repetitive motion structures. While these conventional approaches are capable of effectively handling simple motion sequences or those characterized by fixed periodicity, they prove inadequate when confronted with non-stationary motion sequences encountered in real-world scenarios. In contrast, deep-learning-based approaches [9, 13, 17, 46] have demonstrated remarkable performance improvements. Notably, RepNet [9] and TransRAC [13] leverage temporal similarity matrices of actions to construct models for counting temporal repetitions. However, these similarity-matrix-based methods are not scalable for long videos due to their quadratic computational complexity. Another research line involves

predicting the start and end points of each cycle [46] from coarse to fine. Nevertheless, its practicality is hindered by the requirement for over 30 forward passes to count iteratively from a single video. In this paper, we introduce an effective action cycle representation by leveraging a Transformer encoder-decoder, which reduces the computational complexity from quadratic to linear and demonstrates superior performance in handling both fast and slow actions.

2.2 Temporal Action Detection

The field of temporal action detection [5, 20, 30, 44, 47] is typically classified into two categories: anchor-based methods, and anchor-free methods. Anchor-based methods [18, 28, 43] generate multiple anchors, subsequently classifying these anchors to determine the action boundaries. Anchor-free methods [2, 19, 34, 42] predict action instances by directly regressing the boundary and the center point of an action instance. With the rapid development of Transformer technology, DETR [3] is introduced for object detection task [21, 26, 45, 48] and gains increasing popularity with promising performance. This paradigm promotes the study in many fields such as the action detection tasks [22, 36, 39, 41]. These methods establish a direct connection between action queries and the predicted action instances, enabling them to accurately predict the temporal boundaries of actions. Inspired by these promising results, we explore the possibility of utilizing a novel action query to represent the action cycle in TRC task. In contrast to existing action detection methods, our approach allows the model to capture the inherent repetitive content of an action cycle without relying on predefined class labels and effectively addresses confounding factors such as non-repetitive video backgrounds. This makes our approach well-suited for tackling the challenges of the TRC problem.

3 Method

3.1 Overview

Given an RGB video sequence \mathbf{V} with T frames, The TRC task aims to predict an integer N indicating the number of estimated repetitive action cycles. Our model consists of a video backbone network $\Phi(\cdot)$, a Transformer network with encoder $\mathcal{E}(\cdot)$, decoder $\mathcal{D}(\cdot)$, and multiple prediction heads as shown in Fig. 2. The backbone network $\Phi(\cdot)$ takes a sequence of T video frames as input and extracts feature vectors $\mathbf{F} \in \mathbb{R}^{T \times C}$ for each frame, where C denotes the feature dimension. In practice, we utilize the commonly-used backbone works, *e.g.* TSN [40], and freeze the backbone parameters.

We then design a Transformer encoder-decoder architecture to process the features \mathbf{F} to detect each action cycle instance and obtain the final action cycle count value N . This requires the model to discern each detected action cycle class \mathbf{C}^{cls} and its time position \mathbf{P} . To achieve this, we introduce the concept of *action queries* within the decoder $\mathcal{D}(\cdot)$, which are comprised of *content queries* $\mathbf{Q}^{\text{cnt}} \in$

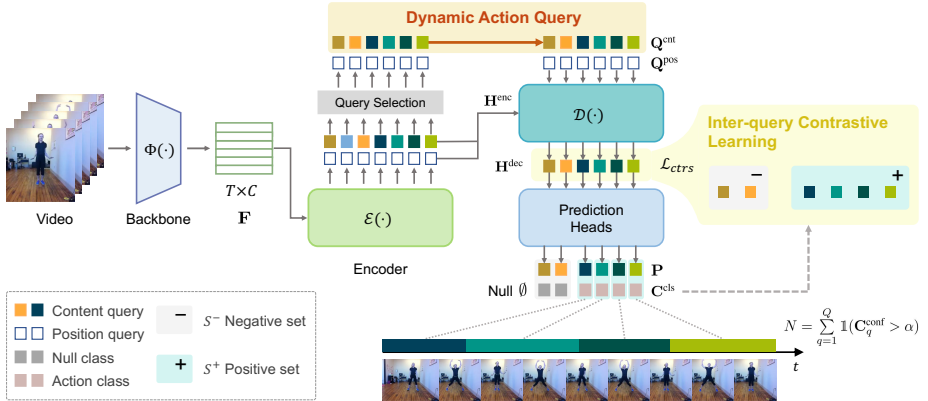


Fig. 2: Framework overview. Given a video input, we first extract video features \mathbf{F} with the backbone network $\Phi(\cdot)$. Then we leverage a Transformer encoder-decoder network to process the features \mathbf{F} to detect each action cycle instance by predicting its action class label \mathbf{C}^{cls} and its time position \mathbf{P} . To tackle the challenge of open-set action categories, we propose **Dynamic Action Query (DAQ)**, allowing the method to attend to the “action of interest” based on the input video contents in a dynamic and contextually aware manner. To recognize actions with identical content, we propose **Inter-query Contrastive Learning (ICL)** to group the “action of interest” and be separated apart from noise actions (*e.g.* background or distractions). Integrating DAQ and ICL, our method can identify contextually similar action instances that are adaptively conditioned on the video content, without manual action class definition. By counting the queries classified as the “action of interest” with classification confidence score \mathbf{C}^{conf} exceeding the threshold α , we finally get the total count value N .

$\mathbb{R}^{Q \times C}$ and *position queries* $\mathbf{Q}^{\text{pos}} \in \mathbb{R}^{Q \times C}$, where Q represents the number of queries. Refer to Fig. 2 for illustration. The content queries \mathbf{Q}^{cnt} are responsible for capturing the action category, while the position queries \mathbf{Q}^{pos} handle the action interval estimation. We use two prediction heads including a classification head and a position head after the decoder to predict the class label \mathbf{C}^{cls} and time position \mathbf{P} for each query, respectively.

To tackle the challenge of open-set action categories, we define $K = 2$ classes, namely “action of interest” and “null (\emptyset)”. We then propose the **Dynamic Action Query (DAQ)** strategy which adaptively updates the content query \mathbf{Q}^{cnt} of the decoder using distilled content features that are selected from the encoder $\mathcal{E}(\cdot)$. This mechanism eliminates the need for a manual definition of the specific semantics of “action of interest” and allows the decoder to attend to the “action of interest” conditioned on the input video contents in a dynamic and contextually-aware manner. Nevertheless, videos may contain distracting factors such as background elements or other noise actions, necessitating that the detected “action of interest” instances exhibit identical or similar contents. To this end, we propose **Inter-query Contrastive Learning (ICL)** to cluster content queries into positive action set (S^+) and negative null set (S^-) based on

their predicted class label \mathbf{C}^{cls} . Integrating DAQ and ICL allows our method to identify contextually similar action instances that are adaptively based on the video content, and exclude other distracting actions at the same time. Finally, by counting the queries classified as the ‘‘action of interest’’ with classification confidence score \mathbf{C}^{conf} exceeding a threshold α , we get the total count value N .

3.2 Model Architecture

Encoder. The encoder $\mathcal{E}(\cdot)$ is a classical Transformer [39] architecture which processes the video features \mathbf{F} extracted by the backbone network. The output features \mathbf{H}^{enc} of $\mathcal{E}(\cdot)$ will then be fed into a query selection module to select Q queries to be the initial content queries \mathbf{Q}^{cnt} for the decoder. For clarity, we will detail the query selection module later in this section. At now, it can be considered as a rough filter that selects top- Q relevant features as the input queries for decoder $\mathcal{D}(\cdot)$.

Decoder. The decoder $\mathcal{D}(\cdot)$ is also a classical Transformer [39] architecture, which takes the encoder features \mathbf{H}^{enc} and two types of action queries as input and outputs a processed feature $\mathbf{H}^{\text{dec}} \in \mathbb{R}^{Q \times C}$. The action queries are constructed by *content queries* $\mathbf{Q}^{\text{cnt}} \in \mathbb{R}^{Q \times C}$ and *position queries* $\mathbf{Q}^{\text{pos}} \in \mathbb{R}^{Q \times C}$, where \mathbf{Q}^{cnt} and \mathbf{Q}^{pos} are designed for representing the content features and the time position of each action cycle, respectively. The content queries \mathbf{Q}^{cnt} are directly initialized from the distilled content features selected from the encoder $\mathcal{E}(\cdot)$, *i.e.* the proposed DAQ strategy, which will be detailed in Sec. 3.3. The position queries \mathbf{Q}^{pos} are initialized as learnable parameters and transformed to the initial time position $\mathbf{P}^{\text{init}} = (\mathbf{m}^{\text{init}}, \mathbf{d}^{\text{init}}) \in \mathbb{R}^{Q \times 2}$ with a linear layer before feeding into the decoder $\mathcal{D}(\cdot)$, where we propose to use the midpoint \mathbf{m} and the period duration \mathbf{d} to denote each action time position. For clarity, we omit the linear layer in Fig. 2.

Prediction heads. The prediction heads consist of a classification head network and a position head network, which are both MLPs.

The classification head takes the output features of the decoder \mathbf{H}^{dec} as input and predicts the action class label for each content query. Given that the action category is an open set and not preset, we set the number of classes K to be 2 in the classification head, indicating whether it is an ‘‘action of interest’’ or a ‘‘null (\emptyset)’’ class. The classification head employs the Softmax function to calculate the probabilities \mathbf{C}^{cls} of K categories for each action query. We then designate the category with the highest probability as the predicted class label for the respective action query. Subsequently, we regard this probability value as the estimated confidence score \mathbf{C}^{conf} . We define an action query instance as ‘‘action of interest’’ when its confidence score \mathbf{C}^{conf} is higher than the threshold α .

We apply binary Cross-entropy loss to supervise the predicted class labels \mathbf{C}^{cls} for each action instance, aiming to guide the model in effectively discrimi-

nating the action instances of interest from others:

$$\mathcal{L}_{\text{cls}} = \sum_{q=1}^Q \text{CrossEntropyLoss} \left(\mathbf{C}_q^{\text{cls}}, \tilde{\mathbf{C}}_q^{\text{cls}} \right) = \sum_{q=1}^Q \sum_{i=1}^K -\tilde{c}_{q,i} \log(c_{q,i}), \quad (1)$$

where $\mathbf{C}_q^{\text{cls}} = [c_{q,1}, c_{q,2}, \dots, c_{q,K}] \in \mathbb{R}^K$ represents the predicted class label for q^{th} action query. $\tilde{\cdot}$ denotes the GT label.

The position head estimates the residual of the midpoint and duration based on the decoder features \mathbf{H}^{dec} for each query, and adds to the initial time position \mathbf{P}^{init} to get the final estimated time position. We supervise the predicted time positions with L_1 loss and gIoU [31] loss:

$$\mathcal{L}_{\text{pos}} = \sum_{q=1}^Q \left\| \mathbf{P}_q - \tilde{\mathbf{P}}_q \right\| + \lambda_{\text{gIoU}} \sum_{q=1}^Q \left(1 - \text{gIoU}(\mathbf{P}_q, \tilde{\mathbf{P}}_q) \right), \quad (2)$$

where $\mathbf{P}_q = (\mathbf{m}_q, \mathbf{d}_q)$ represents the predicted action instance position for the q^{th} query. $\tilde{\cdot}$ stands for GT label.

Note that the Q predicted instances from the prediction heads are in a random order. Therefore, before applying the two loss terms, we have to establish a one-to-one correspondence between the disordered predicted instances and the ground-truth (GT) labels. Concretely, we employ the Hungarian matching algorithm [15] and the matching process considers two criteria: 1) the action class label is the ‘‘action of interest’’, and 2) the time position of the action must align with a corresponding ground-truth time position label. A matching cost matrix is constructed based on these criteria. For the first criterion, the Negative Log-Likelihood (NLL) loss is employed to assess classification accuracy. For the second aspect, both Intersection over Union (IoU) and L_1 distance are utilized to compute costs, measuring the alignment between the estimated time positions and GT labels. The matching cost matrix is of dimensions $Q \times N_{gt}$, where N_{gt} represents the number of GT action instances. Utilizing the Hungarian matching algorithm [15] based on this cost matrix, we derive the prediction-to-GT matching results.

Query selection. As we mentioned above, videos may contain multiple action categories or other distracting factors such as background elements, therefore, we design a query selection module after the encoder $\mathcal{E}(\cdot)$ to filter the ‘‘action of interest’’ coarsely. To achieve this, we reuse the two prediction heads to predict the class labels and time positions for the output features \mathbf{H}^{enc} of the encoder $\mathcal{E}(\cdot)$. Based on their predicted confidence scores \mathbf{C}^{conf} , the query selection module selects top- Q queries with high confidence that are classified as the ‘‘action of interest’’ to be the initial content queries \mathbf{Q}^{cnt} for the decoder. For clarity, we omit the encoder prediction heads in Fig. 2.

Note that the two prediction head networks are shared between the encoder and decoder. In addition, we apply corresponding supervision using \mathcal{L}_{cls} and \mathcal{L}_{pos} to the encoder prediction heads. Additional experimental results of the encoder prediction heads can be found in the supplementary materials.

3.3 Dynamic Action Query

As discussed in Sec. 1, the TRC problem requires recognizing *open-set* action instances depending on the video content, where the action category is not pre-defined. Therefore, we propose the *Dynamic Action Query* strategy, which adaptively updates the content query \mathbf{Q}^{cnt} using distilled content features from the encoder. Simple yet effective, the DAQ strategy directly initializes the input content queries \mathbf{Q}^{cnt} of the decoder using the Q content queries filtered by the query selection module, as shown in Fig. 2. This mechanism provides priors for the decoder that allows it to attend to the ‘‘action of interest’’ conditioned on the input video contents in a dynamic and contextually aware manner. In this way, we avoid the need for the manual definition of the action categories, thereby improving the models’ generalization capability.

Furthermore, we extensively explore different methods for initializing the queries in the decoder $\mathcal{D}(\cdot)$ in the supplementary material, confirming the DAQ strategy as the most effective.

3.4 Inter-query Contrastive Learning

Since the input video may contain multiple action categories and other distractors such as the background motion, another unique challenge to the TRC task is to recognize action instances with *identical* content. This requires that the actions of interest we classify exhibit similarity in their motion patterns, while other action queries should have dissimilar representations. To tackle this challenge, we propose *Inter-query Contrastive Learning* to distinguish the action queries. Intuitively, we hope to partition the content queries into $K = 2$ main categories through contrastive learning. One category comprises the ‘‘actions of interest’’, with similar representations, while the other consists of null instances. The latter may encompass interfering actions or background elements, with distinct representations from those of the actions of interest.

Concretely, we designate the Q decoder features \mathbf{H}^{dec} features classified into two sets according to the predicted class labels \mathbf{C}^{cls} , as shown in Fig. 2. The features that are classified as actions of interest form the positive set S^+ , while the remaining features form the negative set S^- . Then we apply contrastive learning using InfoNCE loss [12] over the feature space:

$$\begin{aligned} \mathcal{L}_+ &= \sum_{s \in S^+, s \neq q} \exp(\mathbf{H}_q^{\text{dec}} \cdot \mathbf{H}_s^{\text{dec}}) / \tau, & \mathcal{L}_- &= \sum_{s \in S^-} \exp(\mathbf{H}_q^{\text{dec}} \cdot \mathbf{H}_s^{\text{dec}}) / \tau, \\ \mathcal{L}_{\text{ctrs}} &= - \sum_{q \in S^+} \log \left(\frac{\mathcal{L}_+}{\mathcal{L}_+ + \mathcal{L}_-} \right), \end{aligned} \quad (3)$$

where τ is the temperature parameter, and \cdot denotes inner product.

3.5 Training Loss

The overall loss function is defined as:

$$\mathcal{L} = \lambda_{\text{cls}} \mathcal{L}_{\text{cls}} + \lambda_{\text{pos}} \mathcal{L}_{\text{pos}} + \lambda_{\text{ctrs}} \mathcal{L}_{\text{ctrs}}, \quad (4)$$

where λ_{cls} , λ_{pos} , λ_{ctrs} are the coefficients of each loss term, respectively.

4 Experiments

4.1 Datasets and Metrics

RepCountA dataset [13] is currently the largest and most challenging benchmark for the video TRC task ³. It is primarily compiled from fitness videos on YouTube, including a wide range of fitness activities conducted in diverse settings, including homes, gyms, and outdoor environments. This dataset stands out due to its extensive video lengths, significant variations in the average motion cycle, and a higher number of repetitive cycles compared to prior datasets [9, 17, 32, 46]. We use the start and end positions of each action instance \mathbf{P}_q provided by the annotations, and disregard the class action labels. We train our model on the RepCountA train set and select the best model on the validation set. We report the evaluation results on the test set.

UCFRep dataset [46] is a subset of the UCF101 dataset [35], including fitness videos and daily life videos. Following previous work [13], we do not use the train set but directly test our model on the test set to evaluate the model generalization ability.

Metrics. We compute two commonly used metrics, OBO and MAE [9, 13, 46], to evaluate the model performance. **OBO** (Off-By-One count error) measures the percentage that the predicted count is within the GT count ± 1 range. **MAE** (Mean Absolute Error) measures the normalized absolute difference between the predicted and GT counts. Formally,

$$\text{OBO} = \frac{1}{M} \sum_{i=1}^M \left| N_i - \hat{N}_i \leq 1 \right|, \quad \text{MAE} = \frac{1}{M} \sum_{i=1}^M \frac{|N_i - \hat{N}_i|}{N_i}, \quad (5)$$

where N_i and \hat{N}_i are the predicted and GT counts for the i^{th} test video, respectively, and M is the total number of test videos.

To better evaluate the performance of different models in recognizing actions with varying periods, we expand the evaluation metrics with three variants for the OBO and MAE metrics. We split the test video set into three categories based on the average single action period length: short-, medium-, and long-period test sets. We define videos with an average single action duration of fewer than 30 frames as belonging to the short-period test set, videos with an average action duration longer than 60 frames as the long-period test set, and the remaining videos as belonging to the medium-period test set. We compute the OBO and MAE metrics on each of these sets separately.

³ The RepCountB [13] test subset is proprietary and not publicly available.

Table 1: Comparison to the state-of-the-arts on RepCountA [13] dataset. We further calculate MAE and OBO metrics for short-, medium-, and long-period test actions. † denotes action detection approaches.

	Backbone	MAE ↓	OBO ↑	MAE _s ↓	OBO _s ↑	MAE _m ↓	OBO _m ↑	MAE _l ↓	OBO _l ↑
X3D [10]	X3D	0.9105	0.1059	-	-	-	-	-	-
TANet [24]	TANet	0.6624	0.0993	-	-	-	-	-	-
VideoSwinT [23]	Swin-T	0.5756	0.1324	-	-	-	-	-	-
GTRM [14]	I3D	0.5267	0.1589	-	-	-	-	-	-
RepNet [9]	ResNet-50	0.5865	0.2450	0.7793	0.0930	0.5893	0.1591	0.4549	0.4062
Zhang <i>et al.</i> [46]	3D-ResNext101	0.8786	0.1554	-	-	-	-	-	-
TransRAC [13]	Swin-T	0.4891	0.2781	0.5789	0.0233	0.4696	0.2955	0.4420	0.4375
TadTR [22] †	I3D	1.1314	0.0662	0.8364	0.0233	1.1591	0.0000	1.3106	0.1406
ActionFormer [44] †	I3D	0.4990	0.2781	0.4164	0.1628	0.3768	0.3409	0.6385	0.3125
ReAct [33] †	TSN	0.4592	0.3509	0.2805	0.1576	0.3037	0.4318	0.6862	0.3906
Ours	TSN	<u>0.2809</u>	<u>0.4570</u>	<u>0.2411</u>	0.1628	0.1792	<u>0.5455</u>	<u>0.3776</u>	<u>0.5938</u>
Ours	I3D	0.3305	0.4437	0.2421	<u>0.2093</u>	0.2012	0.5227	0.4788	0.5469
Ours	ViT-B	0.2622	0.5430	0.2257	0.2558	<u>0.2002</u>	0.5909	0.3294	0.7031

4.2 Implementation Details

We implement our approach with different backbone video feature extractors respectively, including TSN [40], I3D [4], and ViT-B [8]. For the Transformer architecture, we employ a 2-layer encoder and a 4-layer decoder, both with 8-head attention mechanisms. The feature dimension is set to $C = 512$. We set $Q = 40$ queries in our method empirically. For more results with different feature channels C and query numbers Q , please refer to the supplementary materials. The length of the video input is set to $T = 512$ frames without down-sampling. We utilize the AdamW optimizer [25] with a learning rate of 0.002, a batch size of 64, and train the model for 80 epochs. We set $\lambda_{cls} = 1.0$, $\lambda_{pos} = 5.0$, $\lambda_{gIoU} = 0.4$, $\lambda_{ctrs} = 1.0$, confidence threshold $\alpha = 0.2$. We provide further implementation details in the supplementary.

4.3 Comparison to State-of-the-arts

Results on RepCountA dataset. We compare our proposed approach to the state-of-the-art methods on the RepCountA [13] dataset. We compare with the SOTA action recognition [10, 23, 24], action segmentation [14], and TRC [9, 13, 46] approaches as explored in TransRAC [13]. We further adapt recent DETR-style action detection approaches [22, 33, 44] for the TRC task. We change their output layers accordingly and train them on RepCountA.

As shown in Tab. 1, our approach significantly outperforms the state-of-the-art methods across actions of varying lengths. Specifically, the similarity-matrix-based methods [9, 13] suffer from quadratic computation complexity. To manage this, they employ a sparse sampling strategy, ensuring reasonable content coverage within a limited temporal context window. However, this approach results in inferior performance for short, rapid action instances, as it tends to overlook the cycles. Conversely, the action detection approaches [22, 33, 44] are primarily developed for detecting action instances specific to particular classes.

Table 2: Generalization comparison on UCFRep [46] dataset. We calculate MAE and OBO metrics for short-, medium-, and long-period test actions.

	Backbone	MAE ↓	OBO ↑	MAE _s ↓	OBO _s ↑	MAE _m ↓	OBO _m ↑	MAE _l ↓	OBO _l ↑
RepNet [9]	ResNet-50	<u>0.5336</u>	0.2984	0.6219	0.1739	<u>0.4825</u>	0.3600	0.4996	0.5000
TransRAC [13]	Swin-T	0.6180	0.3143	0.6296	<u>0.1951</u>	0.5842	<u>0.4250</u>	0.6784	0.4118
Ours	TSN	0.6016	0.2959	0.7069	0.0488	0.5777	<u>0.4250</u>	0.4039	0.5882
Ours	I3D	0.5194	<u>0.3980</u>	0.4945	0.2195	0.5865	<u>0.4250</u>	<u>0.4216</u>	0.7647
Ours	ViT-B	0.5435	0.4184	<u>0.5657</u>	<u>0.1951</u>	0.4625	0.5500	0.6804	<u>0.6471</u>

Table 3: Comparison of computational complexity.

	T	Params (M)	FLOPs (G)
RepNet [9]	64	20.47	92.40
TransRAC [13]	64	14.43	100.19
Ours	64	18.87	1.44
Ours	512	18.87	6.06

To adapt them to the TRC task, we modify their output layer to incorporate class-agnostic supervision accordingly. However, relying solely on class-agnostic supervision does not provide them with the ability to dynamically identify repetitive cycles based on the input videos. As a result, their performance on long, slow action instances is generally inferior compared to dedicated TRC approaches. In contrast, our approach effectively balances the detection of actions at various speeds.

Results on UCFRep dataset. We also evaluate the generalization ability of our method. Following previous work [13], we evaluate the model trained on the RepCountA dataset [13] on UCFRep [46] test set. Tab. 2 shows that our approach generally outperforms existing works, with more significant improvements observed in longer-period actions. The results demonstrate the effectiveness and generalization capability of our method.

Efficiency. Additionally, we evaluate the computational complexity of our method in comparison to state-of-the-art methods. We benchmark all the methods with inference on the RepCountA dataset. For fairness of comparison, we calculate the Floating Point Operations (FLOPs) in the counting module for all the methods, excluding the video feature extraction process. We set the batch size to be 1 and clip length to be 64 for each method. Tab. 3 shows that our query-based method significantly reduces the computation load compared to the previous similarity-matrix-based methods [9, 13], while also delivering superior accuracy. Importantly, the difference in computational demand is expected to widen with longer input clip lengths. This is because the computational complexity for similarity-matrix-based methods increases quadratically, whereas it grows linearly in our approach. Unfortunately, due to computational limitations, we are unable to obtain the results of RepNet [9] and TransRAC [13] when $T = 512$.

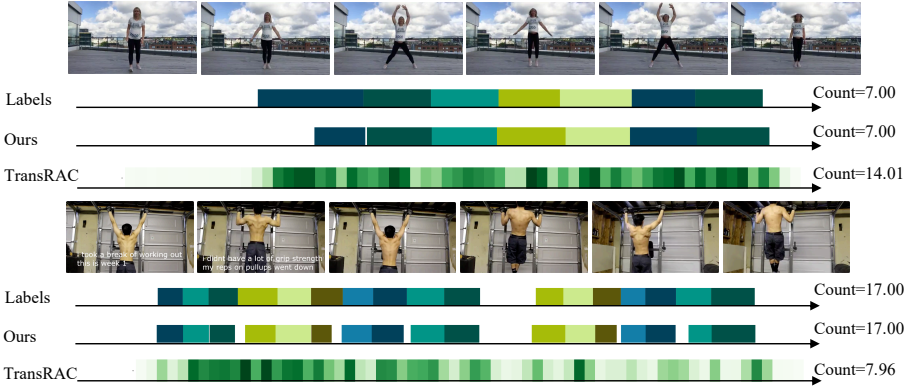


Fig. 3: RepCountA visualization results. Each colored block represents a GT or predicted action instance. TransRAC represents the results by density map, and the final count value is obtained by summing the values in the density map.

4.4 Qualitative Results

We visualize the predictions of our approach and baseline method TransRAC [13] on the RepCountA [13] dataset to better demonstrate our performance improvement in Fig. 3. TransRAC [13] represents action cycles using density maps, and the final count value is obtained by summing the values in the density map. However, this approach suffers from a lack of interpretability and finally results in miscounting. In contrast, our approach not only produces an accurate final count but also precisely localizes the action start and end positions (colored blocks) in most cases, aligning with the GT labels. It can be seen that our method exhibits robustness to changes in viewpoint, background noise, and sudden interruptions. For instance, in the second case of Fig. 3, we accurately and robustly estimate the time positions even with viewpoint changes as well as a sudden interruption in the middle of the timeline.

In addition, our query-based representation offers excellent interpretability, making it easy to identify the issues in case of failures. For example, Fig. 4 shows a typical failure case. Due to the excessive zooming in, the legs of the human body are truncated, making a large difference in the action motion feature, and resulting in several missed cycle counts.

We further illustrate the generalization performance of the proposed method on the unseen UCFRep [46] test set in Fig. 5. We directly apply our trained model and do not use UCFRep training data. Our model still accurately recognizes the action instances and gets the correct count in the challenging cases, indicating robust generalization ability. Specifically, the top case exhibits extreme viewpoint and lighting conditions, while the bottom case contains the action of soccer juggling which is not seen in the training set. We attribute the performance advantage to the proposed DAQ and ICL designs, which empower the model to adaptively adjust the action queries based on the input video features and effectively localize similar (repetitive) action instances, distinguishing



Fig. 4: Visualization of failure case on RepCountA [13] dataset. Due to the excessive zooming in, the legs of the human body are truncated, making a large difference in the action motion feature, and resulting in several missed cycle counts. Each colored block represents a GT or predicted action instance.

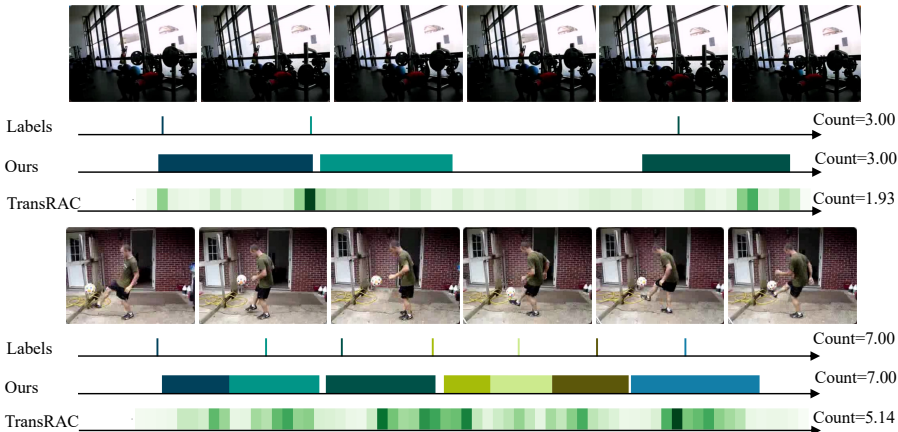


Fig. 5: UCFRep visualization results. Each colored block represents a GT or predicted action instance. TransRAC represents the results by density map, and the final count value is obtained by summing the values in the density map. The vertical lines in the labels represent the time points at which the actions begin since only the starting point annotations are provided in UCFRep [46].

them from the background noise actions. Please refer to our supplementary video for more qualitative results which are robust to varying cycle lengths, sudden interruptions, and multiple distracting action classes.

4.5 Ablation Study

Effect of DAQ and ICL. We implement two ablated models to study the efficacy of the proposed DAQ and ICL designs. Tab. 4 presents the results on RepCountA [13] using the TSN backbone. In ablation (a), we substitute the proposed DAQ module with a static content query, where the content queries \mathbf{Q}^{cnt} are also learnable variables, instead of using the content queries filtered out by the encoder and query selection modules. In ablation (b), we eliminate the ICL design among the action queries. The results demonstrate that both DAQ and ICL contribute to performance improvement, particularly in terms of counting medium and long actions.

Table 4: Effect of DAQ and ICL modules on RepCountA [13] dataset. (a) ablates DAQ strategy. (b) ablates the ICL strategy. (c) is our full model.

	MAE ↓	OBO ↑	MAE _s ↓	OBO _s ↑	MAE _m ↓	OBO _m ↑	MAE _l ↓	OBO _l ↑
(a) <i>w/o</i> DAQ	<u>0.3542</u>	<u>0.4172</u>	0.2624	0.2093	<u>0.2515</u>	<u>0.5227</u>	<u>0.4864</u>	0.4844
(b) <i>w/o</i> ICL	0.4035	0.4040	<u>0.2448</u>	0.2093	0.3106	0.4545	0.5740	<u>0.5000</u>
(c) Ours (full)	0.2809	0.4570	0.2411	<u>0.1628</u>	0.1792	<u>0.5455</u>	0.3776	0.5938

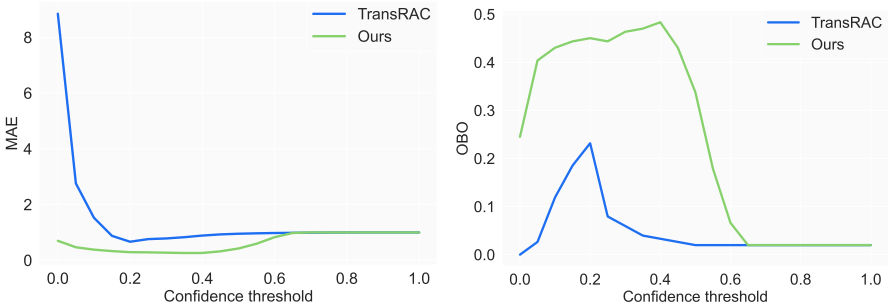


Fig. 6: Results of different confidence thresholds of our method and TransRAC [13]. We depict the MAE (left) and OBO (right) curves of our method (green curve) and the TransRAC (blue curve) approach with regard to different confidence thresholds. The metrics of TransRAC are obtained by binarizing the density map of TransRAC output and then summing to obtain the final count.

Confidence threshold α . We evaluate the impact of different confidence thresholds for the “action of interest” on the final counting results in Fig. 6 (green curve). The results indicate that setting the threshold within the range of 0.2 to 0.4 yields similar performance for our method. Our method consistently outperforms TransRAC [13] (blue curve) by a considerable margin.

5 Conclusion

In conclusion, our study introduces an innovative perspective for the TRC task, which reduces the computational complexity and maintains robustness across varying action periods and video lengths. To tackle the challenge of open-set action categories, we propose DAQ, which improves generalization across different actions. To recognize actions with identical content, we propose ICL, which facilitates learning repetitive action representations and distinguishing them from distractions. Integrating DAQ and ICL, our method can identify contextually similar action instances that are adaptively conditioned on the video content. Experimental results on challenging benchmarks demonstrate the superiority of our approach compared to SOTAs, in terms of both accuracy and efficiency. Furthermore, our approach adeptly balances the demands of diverse action speeds and video durations, establishing a solid foundation for practical implementations in real-world scenarios.

References

1. Azy, O., Ahuja, N.: Segmentation of periodically moving objects. In: 2008 19th International Conference on Pattern Recognition. pp. 1–4. IEEE (2008)
2. Buch, S., Escorcia, V., Ghanem, B., Fei-Fei, L., Niebles, J.C.: End-to-end, single-stream temporal action detection in untrimmed videos. In: Proceedings of the British Machine Vision Conference 2017. British Machine Vision Association (2019)
3. Carion, N., Massa, F., Synnaeve, G., Usunier, N., Kirillov, A., Zagoruyko, S.: End-to-end object detection with transformers. In: Computer Vision–ECCV 2020: 16th European Conference, Glasgow, UK, August 23–28, 2020, Proceedings, Part I 16. pp. 213–229. Springer (2020)
4. Carreira, J., Zisserman, A.: Quo vadis, action recognition? a new model and the kinetics dataset. In: proceedings of the IEEE Conference on Computer Vision and Pattern Recognition. pp. 6299–6308 (2017)
5. Chao, Y.W., Vijayanarasimhan, S., Seybold, B., Ross, D.A., Deng, J., Sukthankar, R.: Rethinking the faster r-cnn architecture for temporal action localization. In: Proceedings of the IEEE conference on computer vision and pattern recognition. pp. 1130–1139 (2018)
6. Chetverikov, D., Fazekas, S.: On motion periodicity of dynamic textures. In: BMVC. vol. 1, pp. 167–176. Citeseer (2006)
7. Cutler, R., Davis, L.S.: Robust real-time periodic motion detection, analysis, and applications. *IEEE Transactions on Pattern Analysis and Machine Intelligence* **22**(8), 781–796 (2000)
8. Dosovitskiy, A., Beyer, L., Kolesnikov, A., Weissenborn, D., Zhai, X., Unterthiner, T., Dehghani, M., Minderer, M., Heigold, G., Gelly, S., Uszkoreit, J., Houshy, N.: An image is worth 16x16 words: Transformers for image recognition at scale. In: International Conference on Learning Representations (2021), <https://openreview.net/forum?id=YicbFdNTTy>
9. Dwibedi, D., Aytar, Y., Tompson, J., Sermanet, P., Zisserman, A.: Counting out time: Class agnostic video repetition counting in the wild. In: Proceedings of the IEEE/CVF conference on computer vision and pattern recognition. pp. 10387–10396 (2020)
10. Feichtenhofer, C.: X3d: Expanding architectures for efficient video recognition. In: Proceedings of the IEEE/CVF conference on computer vision and pattern recognition. pp. 203–213 (2020)
11. Fieraru, M., Zanfir, M., Pirlea, S.C., Olaru, V., Sminchisescu, C.: Aifit: Automatic 3d human-interpretable feedback models for fitness training. In: Proceedings of the IEEE/CVF Conference on Computer Vision and Pattern Recognition. pp. 9919–9928 (2021)
12. He, K., Fan, H., Wu, Y., Xie, S., Girshick, R.: Momentum contrast for unsupervised visual representation learning. In: Proceedings of the IEEE/CVF conference on computer vision and pattern recognition. pp. 9729–9738 (2020)
13. Hu, H., Dong, S., Zhao, Y., Lian, D., Li, Z., Gao, S.: Transrac: Encoding multi-scale temporal correlation with transformers for repetitive action counting. In: Proceedings of the IEEE/CVF Conference on Computer Vision and Pattern Recognition. pp. 19013–19022 (2022)
14. Huang, Y., Sugano, Y., Sato, Y.: Improving action segmentation via graph-based temporal reasoning. In: Proceedings of the IEEE/CVF conference on computer vision and pattern recognition. pp. 14024–14034 (2020)

15. Kuhn, H.W.: The hungarian method for the assignment problem. *Naval research logistics quarterly* **2**(1-2), 83–97 (1955)
16. Laptev, I., Belongie, S.J., Pérez, P., Wills, J.: Periodic motion detection and segmentation via approximate sequence alignment. In: *Tenth IEEE International Conference on Computer Vision (ICCV'05) Volume 1*. vol. 1, pp. 816–823. IEEE (2005)
17. Levy, O., Wolf, L.: Live repetition counting. In: *Proceedings of the IEEE international conference on computer vision*. pp. 3020–3028 (2015)
18. Li, Z., Yao, L.: Three birds with one stone: Multi-task temporal action detection via recycling temporal annotations. In: *Proceedings of the IEEE/CVF Conference on Computer Vision and Pattern Recognition*. pp. 4751–4760 (2021)
19. Lin, C., Xu, C., Luo, D., Wang, Y., Tai, Y., Wang, C., Li, J., Huang, F., Fu, Y.: Learning salient boundary feature for anchor-free temporal action localization. In: *Proceedings of the IEEE/CVF Conference on Computer Vision and Pattern Recognition*. pp. 3320–3329 (2021)
20. Lin, T., Liu, X., Li, X., Ding, E., Wen, S.: Bmn: Boundary-matching network for temporal action proposal generation. In: *Proceedings of the IEEE/CVF international conference on computer vision*. pp. 3889–3898 (2019)
21. Liu, S., Li, F., Zhang, H., Yang, X., Qi, X., Su, H., Zhu, J., Zhang, L.: Dab-detr: Dynamic anchor boxes are better queries for detr. *arXiv preprint arXiv:2201.12329* (2022)
22. Liu, X., Wang, Q., Hu, Y., Tang, X., Zhang, S., Bai, S., Bai, X.: End-to-end temporal action detection with transformer. *IEEE Transactions on Image Processing* **31**, 5427–5441 (2022)
23. Liu, Z., Ning, J., Cao, Y., Wei, Y., Zhang, Z., Lin, S., Hu, H.: Video swin transformer. In: *Proceedings of the IEEE/CVF conference on computer vision and pattern recognition*. pp. 3202–3211 (2022)
24. Liu, Z., Wang, L., Wu, W., Qian, C., Lu, T.: Tam: Temporal adaptive module for video recognition. In: *Proceedings of the IEEE/CVF international conference on computer vision*. pp. 13708–13718 (2021)
25. Loshchilov, I., Hutter, F.: Decoupled weight decay regularization. *arXiv preprint arXiv:1711.05101* (2017)
26. Meng, D., Chen, X., Fan, Z., Zeng, G., Li, H., Yuan, Y., Sun, L., Wang, J.: Conditional detr for fast training convergence. In: *Proceedings of the IEEE/CVF International Conference on Computer Vision*. pp. 3651–3660 (2021)
27. Pogalin, E., Smeulders, A.W., Thean, A.H.: Visual quasi-periodicity. In: *2008 IEEE Conference on Computer Vision and Pattern Recognition*. pp. 1–8. IEEE (2008)
28. Qing, Z., Su, H., Gan, W., Wang, D., Wu, W., Wang, X., Qiao, Y., Yan, J., Gao, C., Sang, N.: Temporal context aggregation network for temporal action proposal refinement. In: *Proceedings of the IEEE/CVF conference on computer vision and pattern recognition*. pp. 485–494 (2021)
29. Ran, Y., Weiss, I., Zheng, Q., Davis, L.S.: Pedestrian detection via periodic motion analysis. *International Journal of Computer Vision* **71**, 143–160 (2007)
30. Redmon, J., Divvala, S., Girshick, R., Farhadi, A.: You only look once: Unified, real-time object detection. In: *Proceedings of the IEEE conference on computer vision and pattern recognition*. pp. 779–788 (2016)
31. Rezatofghi, H., Tsoi, N., Gwak, J., Sadeghian, A., Reid, I., Savarese, S.: Generalized intersection over union: A metric and a loss for bounding box regression. In: *Proceedings of the IEEE/CVF conference on computer vision and pattern recognition*. pp. 658–666 (2019)

32. Runia, T.F., Snoek, C.G., Smeulders, A.W.: Real-world repetition estimation by div, grad and curl. In: Proceedings of the IEEE conference on computer vision and pattern recognition. pp. 9009–9017 (2018)
33. Shi, D., Zhong, Y., Cao, Q., Zhang, J., Ma, L., Li, J., Tao, D.: React: Temporal action detection with relational queries. In: Computer Vision–ECCV 2022: 17th European Conference, Tel Aviv, Israel, October 23–27, 2022, Proceedings, Part X. pp. 105–121. Springer (2022)
34. Shou, Z., Chan, J., Zareian, A., Miyazawa, K., Chang, S.F.: Cdc: Convolutional-de-convolutional networks for precise temporal action localization in untrimmed videos. In: Proceedings of the IEEE conference on computer vision and pattern recognition. pp. 5734–5743 (2017)
35. Soomro, K., Zamir, A.R., Shah, M.: Ucf101: A dataset of 101 human actions classes from videos in the wild. arXiv preprint arXiv:1212.0402 (2012)
36. Tan, J., Tang, J., Wang, L., Wu, G.: Relaxed transformer decoders for direct action proposal generation. In: Proceedings of the IEEE/CVF international conference on computer vision. pp. 13526–13535 (2021)
37. Thangali, A., Sclaroff, S.: Periodic motion detection and estimation via space-time sampling. In: 2005 Seventh IEEE Workshops on Applications of Computer Vision (WACV/MOTION’05)-Volume 1. vol. 2, pp. 176–182. IEEE (2005)
38. Tsai, P.S., Shah, M., Keiter, K., Kasparis, T.: Cyclic motion detection for motion based recognition. *Pattern recognition* **27**(12), 1591–1603 (1994)
39. Vaswani, A., Shazeer, N., Parmar, N., Uszkoreit, J., Jones, L., Gomez, A.N., Kaiser, Ł., Polosukhin, I.: Attention is all you need. *Advances in neural information processing systems* **30** (2017)
40. Wang, L., Xiong, Y., Wang, Z., Qiao, Y., Lin, D., Tang, X., Van Gool, L.: Temporal segment networks: Towards good practices for deep action recognition. In: European conference on computer vision. pp. 20–36. Springer (2016)
41. Wang, X., Zhang, S., Qing, Z., Shao, Y., Zuo, Z., Gao, C., Sang, N.: Oadtr: Online action detection with transformers. In: Proceedings of the IEEE/CVF International Conference on Computer Vision. pp. 7565–7575 (2021)
42. Yuan, Z., Stroud, J.C., Lu, T., Deng, J.: Temporal action localization by structured maximal sums. In: Proceedings of the IEEE Conference on Computer Vision and Pattern Recognition. pp. 3684–3692 (2017)
43. Zeng, R., Huang, W., Tan, M., Rong, Y., Zhao, P., Huang, J., Gan, C.: Graph convolutional networks for temporal action localization. In: Proceedings of the IEEE/CVF international conference on computer vision. pp. 7094–7103 (2019)
44. Zhang, C.L., Wu, J., Li, Y.: Actionformer: Localizing moments of actions with transformers. In: European Conference on Computer Vision. LNCS, vol. 13664, pp. 492–510 (2022)
45. Zhang, H., Li, F., Liu, S., Zhang, L., Su, H., Zhu, J., Ni, L.M., Shum, H.Y.: Dino: Detr with improved denoising anchor boxes for end-to-end object detection. arXiv preprint arXiv:2203.03605 (2022)
46. Zhang, H., Xu, X., Han, G., He, S.: Context-aware and scale-insensitive temporal repetition counting. In: Proceedings of the IEEE/CVF Conference on Computer Vision and Pattern Recognition. pp. 670–678 (2020)
47. Zhao, Y., Xiong, Y., Wang, L., Wu, Z., Tang, X., Lin, D.: Temporal action detection with structured segment networks. In: Proceedings of the IEEE international conference on computer vision. pp. 2914–2923 (2017)
48. Zhu, X., Su, W., Lu, L., Li, B., Wang, X., Dai, J.: Deformable detr: Deformable transformers for end-to-end object detection. arXiv preprint arXiv:2010.04159 (2020)